Biomarker screen for efficacy of oncolytic virotherapy in patient-derived pancreatic cancer cultures

Theresa E. Schäfer,[a,b] Lisanne I. Knol,[c,d] Ferdinand V. Haas,[e] Anna Hartley,[f,g] Sophie C. S. Pernickel,[a,b] Attila Jády,[c,d] Maximiliane S. C. Finkbeiner,[e] Johannes Achberger,[e,h] Stella Arelaki,[i] Živa Modic,[a,ab] Katrin Schröer,[e] Wenli Zhang,[e] Barbara Schmidt,[j,k] Philipp Schuster,[k] Sebastian Haferkamp,[l] Johannes Doerner,[m] Florian Gebauer,[m] Maximilian Ackermann,[n,o] Hans-Michael Kvasnicka,[n] Amit Kulkarni,[p] Selas T. F. Bots,[q] Vera Kemp,[q] Lukas J. A. C. Hawinkels,[r] Anna R. Poetsch,[s,t,u,v,w] Rob C. Hoeben,[q] Anja Ehrhardt,[e] Antonio Marchini,[f,p,ac] Guy Ungerechts,[a,x] Claudia R. Ball,[c,d,i,y,z] and Christine E. Engeland[a,e,aa,*]

[a]Clinical Cooperation Unit Virotherapy, German Cancer Research Center (DKFZ), Heidelberg, Germany
[b]Medical Faculty, Heidelberg University, Heidelberg, Germany
[c]Department for Translational Medical Oncology, National Center for Tumor Diseases Dresden (NCT/UCC), A Partnership Between DKFZ, Faculty of Medicine and University Hospital Carl Gustav Carus, TUD Dresden University of Technology, and Helmholtz-Zentrum Dresden - Rossendorf (HZDR), Germany
[d]Translational Medical Oncology, Faculty of Medicine and University Hospital Carl Gustav Carus, TUD Dresden University of Technology, Dresden, Germany
[e]Virology and Microbiology, Center for Biomedical Education and Research (ZBAF), Witten/Herdecke University, Witten, Germany
[f]Laboratory of Oncolytic Virus Immuno-Therapeutics, German Cancer Research Center (DKFZ), Heidelberg, Germany
[g]DNA Vector Laboratory, German Cancer Research Center (DKFZ), Heidelberg, Germany
[h]Institute of Immunology, Faculty of Medicine Carl Gustav Carus, Technische Universität Dresden, Dresden, Germany
[i]German Cancer Research Center (DKFZ) Heidelberg, Translational Functional Cancer Genomics, Germany
[j]Institute of Clinical Microbiology and Hygiene, University Hospital Regensburg, Regensburg, Germany
[k]Institute of Medical Microbiology and Hygiene, University of Regensburg, Regensburg, Germany
[l]Department of Dermatology, University Hospital Regensburg, Regensburg, Germany
[m]Department of Surgery, Helios University Hospital Wuppertal, Wuppertal, Germany
[n]Institute of Pathology and Molecular Pathology, Helios University Clinic Wuppertal, Witten/Herdecke University, Witten, Germany
[o]Institute of Pathology, RWTH University Clinics University Aachen, Aachen, Germany
[p]Laboratory of Oncolytic Virus Immuno-Therapeutics, Luxembourg Institute of Health, Luxembourg
[q]Virus and Cell Biology Lab, Department of Cell and Chemical Biology, Leiden University Medical Center, Leiden, the Netherlands
[r]Department of Gastroenterology and Hepatology, Leiden University Medical Center, Leiden, the Netherlands
[s]Biotechnology Center, Technische Universität Dresden, Dresden, Germany
[t]Faculty of Medicine and University Hospital Carl Gustav Carus, Technische Universität Dresden, Dresden, Germany
[u]Helmholtz-Zentrum Dresden - Rossendorf (HZDR), Dresden, Germany
[v]German Cancer Consortium (DKTK), Partner Site Dresden and German Cancer Research Center (DKFZ), Heidelberg, Germany
[w]National Center for Tumor Diseases (NCT), Dresden, Germany: German Cancer Research Center (DKFZ), Heidelberg, Germany
[x]Department of Medical Oncology, University Hospital Heidelberg, Heidelberg, Germany
[y]German Cancer Consortium (DKTK), Partner Site Dresden, Germany
[z]Faculty of Biology, TUD Dresden University of Technology, Germany
[aa]Experimental Hematology and Immunotherapy, Department of Hematology, Hemostaseology, Cellular Therapy and Infectious Diseases, Faculty of Medicine and Leipzig University Hospital, Fraunhofer Institute for Cell Therapy and Immunology (IZI), Leipzig, Germany

eBioMedicine
2024;105: 105219
Published Online xxx
https://doi.org/10.1016/j.ebiom.2024.105219

Summary

Background Pancreatic ductal adenocarcinoma (PDAC) is a tumour entity with unmet medical need. To assess the therapeutic potential of oncolytic virotherapy (OVT) against PDAC, different oncolytic viruses (OVs) are currently investigated in clinical trials. However, systematic comparisons of these different OVs in terms of efficacy against PDAC and biomarkers predicting therapeutic response are lacking.

Methods We screened fourteen patient-derived PDAC cultures which reflect the intra- and intertumoural heterogeneity of PDAC for their sensitivity to five clinically relevant OVs, namely serotype 5 adenovirus Ad5-hTERT, herpes virus T-VEC, measles vaccine strain MV-NIS, reovirus jin-3, and protoparvovirus H-1PV. Live cell analysis, quantification of viral genome/gene expression, cell viability as well as cytotoxicity assays and titration of viral progeny were

*Corresponding author. Clinical Cooperation Unit Virotherapy, German Cancer Research Center (DKFZ), Heidelberg, Germany.
E-mail addresses: christine.engeland@medizin.uni-leipzig.de, christine.engeland@uni-wh.de, christine.engeland@nct-heidelberg.de (C.E. Engeland).
[ab]Present address: Department of Experimental Oncology, Institute of Oncology Ljubljana, Ljubljana, Slovenia.
[ac]Current address: European Commission, Joint Research Centre (JRC), Geel, Belgium.

conducted. Transcriptome profiling was employed to identify potential predictive biomarkers for response to OV treatment.

Findings Patient-derived PDAC cultures showed individual response patterns to OV treatment. Twelve of fourteen cultures were responsive to at least one OV, with no single OV proving superior or inferior across all cultures. Known host factors for distinct viruses were retrieved as potential biomarkers. Compared to the classical molecular subtype, the quasi-mesenchymal or basal-like subtype of PDAC was found to be more sensitive to H-1PV, jin-3, and T-VEC. Generally, expression of viral entry receptors did not correlate with sensitivity to OV treatment, with one exception: Expression of Galectin-1 (LGALS1), a factor involved in H-1PV entry, positively correlated with H-1PV induced cell killing. Rather, cellular pathways controlling immunological, metabolic and proliferative signaling appeared to determine outcome. For instance, high baseline expression of interferon-stimulated genes (ISGs) correlated with relative resistance to oncolytic measles virus, whereas low cyclic GMP-AMP synthase (cGAS) expression was associated with exceptional response. Combination treatment of MV-NIS with a cGAS inhibitor improved tumour cell killing in several PDAC cultures and cells overexpressing cGAS were found to be less sensitive to MV oncolysis.

Interpretation Considering the heterogeneity of PDAC and the complexity of biological therapies such as OVs, no single biomarker can explain the spectrum of response patterns. For selection of a particular OV, PDAC molecular subtype, ISG expression as well as activation of distinct signaling and metabolic pathways should be considered. Combination therapies can overcome resistance in specific constellations. Overall, oncolytic virotherapy is a viable treatment option for PDAC, which warrants further development. This study highlights the need for personalised treatment in OVT. By providing all primary data, this study provides a rich source and guidance for ongoing developments.

Funding German National Science Foundation (Deutsche Forschungsgemeinschaft, DFG), German Cancer Aid (Deutsche Krebshilfe), German National Academic Scholarship Foundation (Studienstiftung des deutschen Volkes), Survival with Pancreatic Cancer Foundation.

Keywords: Pancreatic cancer; Oncolytic virotherapy; Cancer immunotherapy; Viral vectors

Research in context

Evidence before this study

We searched PubMed and clinicaltrials.gov using the terms "pancreatic cancer", "pancreatic ductal adenocarcinoma (PDAC)", "(oncolytic) virus", and "(oncolytic) virotherapy" without language or geographic restrictions. A variety of different viruses have been tested preclinically as well as clinically for efficacy against PDAC. However, we neither found studies directly comparing the efficacy of different oncolytic viruses nor validating biomarkers for response of PDAC to a specific virotherapeutic. Nevertheless, effective virus-mediated lysis is a prerequisite to fully exploit the immunotherapeutic potential of virotherapy, highlighting the need for predictive signatures in a heterogenous disease such as PDAC.

Added value of this study

We screened fourteen patient-derived PDAC cultures for their sensitivity to five clinically relevant oncolytic viruses (OVs). To our knowledge, this is the first report of a study comparing several OVs and characterising OV dynamics in a single PDAC model system to identify tumour cell-intrinsic factors determining response or resistance to virotherapy. Patient-derived PDAC cultures exhibited individual response patterns to the different OVs, showing that no single OV is superior for treatment of PDAC. We correlated sensitivity to the OVs with transcriptome data to identify potential biomarkers of response. We revealed that PDAC molecular subtype affects response to three of the five OVs tested. We found that not viral entry receptor expression, but cellular pathways controlling immunological, proliferative, and metabolic functions are associated with OV sensitivity.

Implications of all the available evidence

Rather than testing for single biomarkers, the present data suggest that ex vivo sensitivity and transcriptome analysis should be employed for patient stratification. Within the framework of personalised medical oncology, this will allow for selection of patients that will most likely benefit from a specific OV. By providing all primary data, this study can guide future translational efforts to advance virotherapy against PDAC.

Introduction

Despite significant progress in medical oncology over the past decades, advanced-stage pancreatic ductal adenocarcinoma (PDAC) remains a tumour entity with a dismal prognosis.[1] Notwithstanding extensive efforts, survival rates of patients suffering from PDAC have hardly improved. Thus, a number of clinical trials with experimental therapies are underway to address this high unmet medical need. These experimental therapies include oncolytic viruses (OVs). OVs replicate preferentially in malignant cells, ultimately inducing tumour cell death. Furthermore, virus-mediated lysis releases tumour-associated antigens in a highly immunostimulatory context, thereby promoting induction of anti-tumour immunity. While some viruses are naturally oncolytic, most OVs are genetically engineered to confer tumour selectivity and enhance efficacy. No less than 40 OVs from at least ten different virus families have entered clinical development.[2] Thus far, a few OVs have gained regulatory approval, including Oncorine, an adenovirus used for treatment of head and neck cancer in China as well as talimogene laherparepvec (also referred to as T-VEC), a herpes virus approved by the FDA and EMA for treatment of advanced melanoma.[3] However, with the exception of individual cases, OV therapy has not achieved remission of advanced tumours and a prime candidate among all OVs has not emerged so far.[4] Viruses from six different families have been or are currently tested in clinical trials recruiting patients with PDAC (Table S1).

These viruses differ vastly in terms of genome structure and replication cycle, which results in distinct virus-host interactomes with implications for efficacy of virotherapy. However, a systematic assessment and comparison of efficacy of different OVs against PDAC is currently lacking. Therefore, the aim of this study was to provide insights into the anti-tumour activity of five selected OVs using patient-derived PDAC cultures and to eventually identify potential biomarkers associated with sensitivity of PDAC to virotherapy (Fig. S1a).

To this end, we employed five different OVs that are currently in clinical development, including adenovirus (AdV), attenuated measles virus (MV), parvovirus (PV), reovirus (RV), and herpes simplex virus (HSV) derivatives. In this study, Ad5-hTERT, a serotype 5 AdV in which essential (E1) gene expression is under control of the human telomerase reverse transcriptase promoter was used as a representative and well-studied AdV.[5] MV-eGFP and MV-NIS are negative-strand RNA viruses of the MV Edmonston vaccine lineage, engineered to express GFP or human sodium-iodide symporter that allows tracking of MV replication in vitro and in vivo, respectively.[6–8] The rat protoparvovirus H-1PV is a small, unmodified DNA virus.[9,10] RVs are double-stranded RNA viruses with segmented genomes. Here, the RV type 3 Dearing (T3D) strain derivative jin-3 was studied, which exhibits a broader cell tropism than parental T3D and does not depend on Junction-Adhesion Molecule (JAM-A) for cell entry.[11] Talimogene laherparepvec (T-VEC, Imlygic™) an attenuated HSV type 1 engineered to express human GM-CSF, is approved by the FDA and EMA for treatment of advanced melanoma.[12] Characteristics of the viruses are summarised in Fig. 1a.

Several clinical trials investigating the activity of these viruses against PDAC are currently planned or ongoing (Table S1).

Methods

Ethics approval and consent to participate

All experiments with human material were performed in accordance with the Declaration of Helsinki and were approved by the ethics committee of the Medical Faculty of Heidelberg University (323/2004, Amendment 03), the ethics committee of Witten/Herdecke University (118/2021) and the Review Committee Biobank & Biomaterials of Leiden University Medical Center (registration number: RP24.004. All studies with patient material were performed with patients' informed consent.

Consent for publication: Not applicable.

Viruses

Ad5-hTERT was obtained from Florian Kühnel,[14] produced in HEK293 cells and purified by CsCl density gradient centrifugation.[15] MV-NIS was obtained from Imanis Life Sciences, Rochester, MN, USA as a high-titer purified stock. To track viral gene expression, a measles vaccine strain encoding enhanced green fluorescent protein, MV-eGFP, was produced in Vero cells and used for live cell analysis, XTT assay as well as crystal violet staining.[16] H-1PV was produced, purified and titrated by Barbara Leuchs as described previously.[17–20] The reovirus (RV) type 3 Dearing (T3D) strain derivative jin-3 with a broader cell tropism was originally obtained by passaging of wild-type T3D on JAM-A-negative U118MG glioblastoma cells and was produced in 911 cells with subsequent CsCl gradient purification as described previously.[11] Talimogene laherparepvec (Imlygic™; Amgen, Thousand Oaks, CA, USA) was obtained via the pharmacy of Heidelberg University Hospital and propagated for individual experiments as described previously.[21]

Patient-derived PDAC cultures

PDAC cultures were established as described previously.[13] Characteristics of patient tumours are listed in Fig. 1b. Purity of all patient-derived cultures was validated through Multiplexion Cell Contamination Testing (Multiplexion, Heidelberg, Germany).[22] Identity of the cultures was confirmed through SNP analysis by Multiplexion (Supplemental Data–Reagent Validation file).[23] Cultures were grown as described in 13 using CSCN medium: Dulbecco's modified Eagle's medium (DMEM) Advanced F12 medium supplemented with

a

Virus family	Virus name	Purity	Description
Adenovirus (AdV)	Ad5-hTERT	Research grade, CsCl gradient	Serotype 5 Adenovirus expressing the early transcription unit E1 under control of the telomerase promoter.
Parvovirus (PV)	H-1PV	Research grade, iodixanol gradient	Rat protoparvovirus, non pathogenic in humans.
Reovirus (RV)	Jin-3	Research grade, CsCl gradient	JAM-A independent cell entry, Type 3 Dearing strain
Measles virus (MV)	MV-NIS	Clinical grade	Attenuated MV vaccine strain encoding the human thyroidal sodium iodide symporter (NIS), allows tracking of MV replication in vivo
	MV-eGFP	Research grade, Vero cell lysate	Derived from Edmonston B vaccine strain, encoding GFP for tracking in vitro
Herpes-simplex-virus (HSV)	T-VEC	Clinical grade	HSV-1 encoding human GM-CSF, approved for therapeutic use in advanced stage malignant melanoma,

b

Culture identifier	KRAS status	Age	Sex	Histology of patient tumour
PC01	KRASmut	62	Male	Ductal adenocarcinoma
PC03	KRAS G12D	74	Male	Adenosquamous carcinoma
PC06	KRAS G12V	68	Male	Ductal adenocarcinoma
PC07	N/A	76	Female	Ductal adenocarcinoma
PC09	KRASmut	77	Female	Ductal adenocarcinoma
PC10	KRAS G12D	62	Male	Ductal adenocarcinoma
PC12	wt	62	Male	Ductal adenocarcinoma with oncocytic type IPMN
PC17	N/A	69	Male	Ductal adenocarcinoma
PC18	KRASmut	52	Female	Ductal adenocarcinoma
PC20	KRASmut	66	Female	Ductal adenocarcinoma
PC21	KRASmut	72	Male	Ductal adenocarcinoma
PC25	KRASmut	62	Male	Ductal adenocarcinoma
PC28	N/A	63	Female	Ductal adenocarcinoma
PC31	KRAS G12D	60	Male	Ductal adenocarcinoma

c

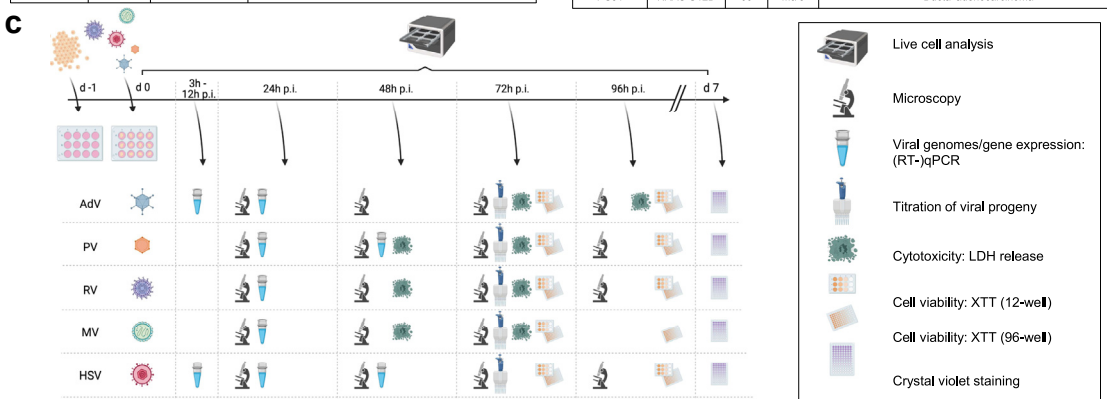

Fig. 1: Screening for sensitivity of PDAC to oncolytic virotherapy a. Characteristics of oncolytic viruses employed in the screen. b. Patient-derived PDAC cultures used in the screen including patient demographics and histology.[13] N/A: Information not available. c. Schematic outline of the screening set-up. Assays and time points are depicted for every oncolytic virus, assays were performed with all 14 cultures listed in (b).

2% B27 supplement, 0.6% glucose, 2 mM L-glutamine (all from Thermo Fisher Scientific, Germany), 12 µg/mL heparin and 5 mM HEPES buffer (both from Sigma Aldrich, Germany). Every 3–4 days, medium was changed and recombinant human (rh) cytokines were added: 10 ng/mL rh fibroblast growth factor (FGF)-basic, 20 ng/mL rhFGF-10, and 20 ng/mL rhNodal (all from R&D Systems, Germany).

Additional PDAC cultures were derived from a patient-derived xenograft (PACX34) and endoscopic-ultrasound (EUS)-guided fine-needle biopsies (PAC1164, PACF005, and PACF002) as described previously[24] with minor modifications as described in Supplementary Methods.

Surgical specimens

Tumour specimens were obtained from patients diagnosed with PDAC undergoing surgery at the Department of General, Visceral and Vascular Surgery, Helios Universitätsklinikum Wuppertal, Germany. Fresh tissue specimens were mechanically dissected, placed in a 50 mL tube containing 20 mL RPMI (PAN Biotech) with 1× penicillin/streptomycin and amphotericin B (ABAM) (Gibco, Thermo Fisher Scientific) and transferred on ice to the laboratory. Average time from surgical removal to the beginning of the tissue dissociation protocol in the laboratory was 60 min. The tissue specimens were cut into 1 mm^3 pieces and resuspended in 20 mL PBS (PAN Biotech) with 1× ABAM. Tissue pieces were washed three times by centrifugation at 300×g for 5 min and resuspension in 25 mL PBS with 1× ABAM. After the final wash, pieces were resuspended in 20 mL digestion medium (RPMI supplemented with 120 µL 25 mM $CaCl_2$ (Carl Roth, Germany), 40 mg/mL Collagenase IV (Sigma, Germany), 5 CU/mL Dispase II (Corning, Thermo Fisher Scientific), 4 µg/mL DNaseI (StemCell, Germany), and 1× ABAM and incubated for 3 h at 37 °C in a water bath. Every 45 min, cells were filtered through a 100 µm filter, pelleted by centrifugation at 300×g for 5 min and resuspended in DMEM with 10% FBS and 1× ABAM. At the last filtering step, filters were washed with PBS twice to extract all cells, and cells were pelleted, resuspended in 6 mL ACK Lysis buffer (Gibco, Thermo Fisher Scientific) and incubated for 5 min at room temperature. Cells were then washed twice using 10 mL PBS with 1× ABAM. 5×10^5 cells in 300 µL CSCN medium with cytokines and 1× ABAM were seeded into Matrigel (Corning, Thermo Fisher Scientific) coated wells of a 24 well-plate in duplicates and infected with the respective virus dose in

100 µL DMEM per well. Viability was assessed 72 h p.i. by XTT assay as described below.

Patients of all genders were eligible to participate in the study. Information on sex and gender was collected as self-reported by study participants.

Cell culture

Vero cells were obtained from the American Type Culture Collection (ATCC, CCL-81; RRID: CVCL_0059) and cultivated in DMEM (Thermo Fisher Scientific) with 10% fetal bovine serum (FBS, PAN Biotech, Germany). HEK293 cells were obtained from the German Collection of Microorganisms and Cell Cultures (DSMZ, ACC 305; RRID: CVCL_0045) and cultivated in DMEM (PAN Biotech, Germany) with 10% FBS (PAN Biotech). Human Embryonic Retinoblasts 911 (911; RRID: CVCL_1K15) described previously[25] were cultivated in DMEM with 10% FBS. NB-324 K human newborn kidney cells[26] (NBK) were cultivated in DMEM with 10% FBS.

PDAC cell lines Capan-I (ATCC, HTB-79; RRID: CVCL_0237), MIA PaCa-2 (ATCC, CRL-1420; RRID: CVCL_0428), AsPC-1 (ATCC, CRL-1682; RRID: CVCL_0152), PANC-1 (ATCC, CRL-1469; RRID: CVCL_0480), BxPC-3 (ATCC, CRL-1687; RRID: CVCL_0186), T3M–4 (from Zahari Raykov; RRID: CVCL_VQ95), IMIM-PC2 (from Stephan A. Hahn; RRID: CVCL_0345), and HPAC (from Daniel Abate-Daga; RRID: CVCL_3517) were cultured in DMEM with 10% FBS. Cells were cultured at 37 °C in humidified incubators with 5% CO_2. Mycoplasma contamination was routinely excluded by PCR testing (VenorGeM Mycoplasma Detection Kit, Minerva Biolabs, Germany). Cell lines were validated by STR profiling (Eurofins Genomics, Germany; Supplemental Data–Reagent Validation file) and DSMZ cell drive as well as CLASTR.[27,28]

Screening of PDAC cultures for sensitivity to virotherapy

Sensitivity of the PDAC cultures was assessed via microscopy, live cell analysis, quantification of viral genomes and viral gene expression,[29,30] viral progeny titration[31] as well as cytotoxicity and cell viability assays (Fig. 1c). Multiplicities of infection (MOIs) and time points for readouts were adjusted following pre-screens for each virus individually and chosen to account for the replication and cytotoxic characteristics of the different OVs. Details are provided in the Supplementary Methods.

For each culture-virus combination, an overall cell viability score was calculated based on the XTT assay. For this, only the infection with the higher MOI for each virus was used. Firstly, the XTT scores for the PDAC cultures at each time point and each well type were scaled by z-score transformation to standardise the distributions. Subsequently, for each culture a weighted average was calculated, with data from 12-well plates counting twice as heavy.

Microarray analysis

RNA was isolated using RNeasy Mini Plus Kit and analyzed using the Affymetrix Human Clariom S (Affymetrix/Thermo Fisher Scientific) by the Microarray Core Facility of the German Cancer Research Center.

Transcriptomics analysis

Transcriptomics analysis was carried out using R. Background subtraction, normalisation, and summarization of the microarray data was carried out with robust multichip average (RMA) using the *affy* package (version 1.70.0).[32] For all further transcriptome analyses, the resulting log2-transformed normalised gene counts were used. K-means clustering was performed with the stats package (version 4.1.0) using k = 3, as this was the number of clusters with the highest silhouette score. Differential expression analysis between the different detected subgroups was carried out using eBayes from the package *limma* (version 3.48.3) with trend = TRUE.[33,34] To determine biological pathways associated with sensitivity to a specific OV, gene set enrichment analysis[35] was carried out with fgseaSimple from the *fgsea* package (version 1.18.0)[36] with 100,000 permutations and HALLMARK[37] gene sets. As input, the Spearman rank correlation between the gene expression and the viability scores for each PDAC culture were used.

For visualisation the R packages ComplexHeatmap (version 2.10.0),[38,39] circlise (version 0.4.13),[40] ggplot2 (version 3.3.5)[41] and the Venny online tool (version 2.1)[42] were used. Spearman's ρ was calculated with GraphPad Prism, version 9.4.1.

Statistics

Correlations of gene expression with viability upon OV treatment were performed using Spearman's rank correlation in GraphPad Prism (version 9.4.1). Differences between two samples (cGAS overexpressing and the respective parental cell line) were analysed using two-sided unpaired t-tests using GraphPad Prism (version 10.2.2), assuming Gaussian distribution and assuming both populations have the same standard deviation. Differences were considered statistically significant if $p < 0.05$.

Role of funders

The funders had no role in the study design, data collection, data analyses, interpretation or writing of the report.

Results

Patient-derived PDAC cultures exhibit differential sensitivity to oncolytic viruses

A set of fourteen patient-derived PDAC cultures which reflect the intra- and intertumoural heterogeneity of this entity[13] were treated with five different clinically relevant

OVs (Fig. 1a and b). Readouts to determine the sensitivity of these cultures to the OVs included microscopy, live cell analysis, quantification of viral genome/gene expression, cell viability and cytotoxicity assays (Fig. 1c). Phase-contrast microscopy revealed differing responses of the individual PDAC cultures to OV infection (Fig. 2a). The five OVs elicited distinct cytopathic effects. Treatment with AdV, PV, and RV resulted in rounding of dying cells, while MV induced syncytia formation and HSV caused cell blebbing, pointing towards different mechanisms of cell death.[43] Moreover, differential sensitivity of the PDAC cultures to OVs was observed: For instance, PC01 seemed fairly resistant to three OVs, but responded to HSV and MV, whereas PC03 as well as PC31 appeared sensitive to all five OVs and PC09 seemed to be sensitive only to AdV and MV to some extent. These observations were confirmed by live cell analysis (Fig. S2). Crystal violet staining of the cultures seven days after treatment showed unique patterns of sensitivity towards the OVs (Fig. 2b). Except for PC18 and PC28, which appeared resistant to all OVs tested, all other PDAC cultures responded to at least one of the five OVs.

As a quantitative readout, reduction in cell viability was chosen as a measure for sensitivity to oncolytic virotherapy and assessed for each culture and virus in two independent experiments (Fig. 2c and Fig. S4). While some cultures, such as PC03 and PC31, responded fairly well to all viruses, PC17 responded well to PV and RV, but seemed to be resistant to AdV. PC09, on the other hand, responded well to AdV, but seemed resistant towards HSV, RV, and PV. PC07 responded best to treatment with PV and seemed resistant to MV. PC25 responded well to HSV and appeared resistant towards MV. PC06, on the other hand, responded only to MV and HSV and was resistant to all other OVs.

Overall, these results indicate that most PDACs are sensitive to at least one clinically relevant OV. However, which OV is most effective seems to depend on individual, tumour-intrinsic factors.

The microenvironment of PDAC is characterised by a dense stromal component, contributing to intra- and inter-patient heterogeneity, impeding the penetration of various anti-tumour agents into the core of the tumour and modulating anti-tumour immune responses.[44,45] To assess susceptibility of primary tumour tissue with

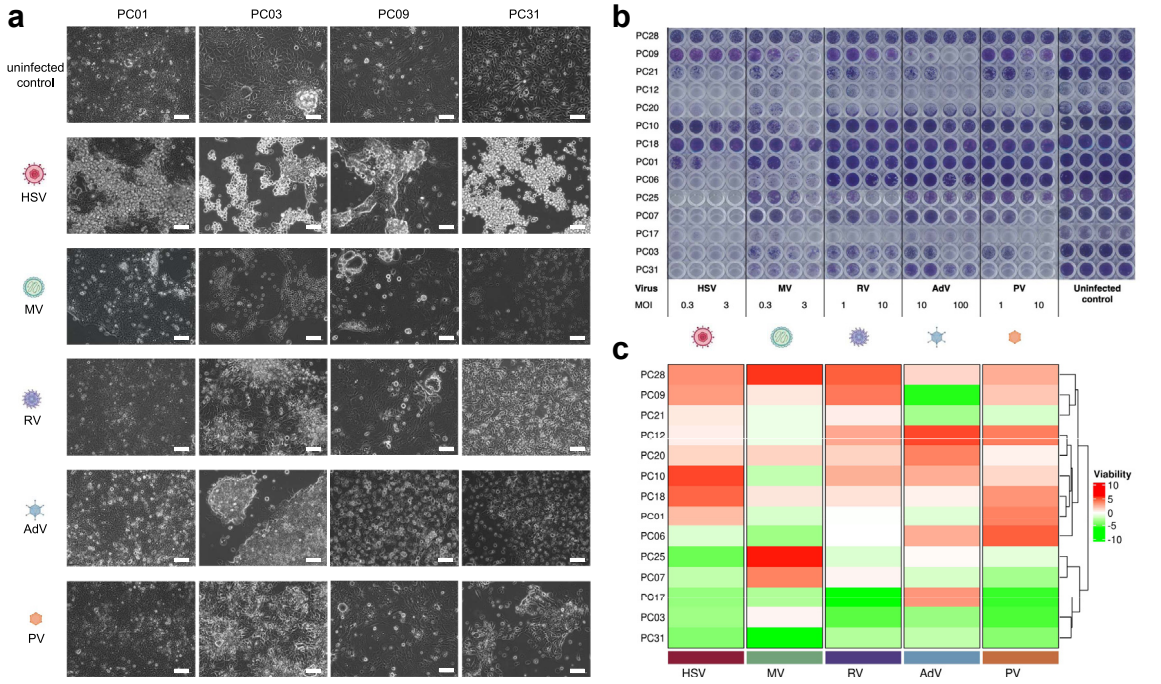

Fig. 2: PDAC cultures exhibit differing responses to OV treatment a. Phase microscopy. Exemplary images for four PDAC cultures (PC01, PC03, PC09, and PC31) are shown. Cells were seeded in 12-well plates and inoculated with HSV (MOI 3), MV (MOI 3), RV (MOI 10), AdV (MOI 100), or PV (MOI 10). Images were acquired 72 h post virus inoculation (p.i.) scale bar: 100 µm. b. Crystal violet staining. Cells from all PDAC cultures were seeded in 96-well plates in parallel and inoculated with HSV (MOI 0.3 and 3), MV (MOI 0.3 and 3), RV (MOI 1 and 10), AdV (MOI 10 and 100), or PV (MOI 1 and 10), in technical duplicates. Crystal violet staining was performed seven days p.i. All culture-virus combinations are shown with two MOIs per virus in technical duplicates. c. Heatmap of the viability score based on the XTT assay for each culture per virus. After seeding in 12- and 96-well plates, PDAC cultures were inoculated with OVs as in (b) and cell viability was determined by XTT assay 72 h and 96 h p.i. (one sample per condition). Viability score was calculated as detailed in Methods. PDAC cultures with a relatively high viability score (red) are relatively resistant to a specific OV, while cultures with a low viability score (green) show relative sensitivity.

a preserved stromal compartment towards the five OVs included in this study, surgical PDAC specimens from four different patients were obtained. The four primary tumour specimens showed varying sensitivity and considerable inter-patient heterogeneity upon treatment with the five OVs. Exemplarily, microscopy images are shown for the infection of tumour tissue from Patients 1 and 4 with MV-GFP in Fig. S3a. Although primary samples showed a high density of stromal cells, infection of tumour cells and syncytia formation were detected via fluorescence microscopy. Proportion of tumour and stroma were evaluated by a trained pathologist, details are shown in Fig. S3b. Viability of the tumour-stroma composite samples was determined and compared to matched uninfected control samples at 72 h post infection (Fig. S3c). Different response patterns were observed across the four patients. Tumour tissue of Patient 2 responded best to OV treatment, while tissue of Patient 3 seemed to be resistant towards all tested OVs with the exception of PV. Tumour tissue of Patient 4 showed a strong response to MV and, to a lesser extent, to RV, but hardly any reduction in cell viability upon treatment with AdV, HSV, and PV. For Patient 1, the response spectrum of the five OVs differed substantially: While RV and HSV elicited a reduction in viability, the tissue seemed to be resistant towards MV and PV.

Five oncolytic viruses elicit distinct response patterns in patient-derived PDAC cultures

Additional parameters addressing several steps of the viral replication cycle were evaluated to characterise OV response kinetics of the PDAC cultures. Viral genome replication and viral gene copies were assessed using established (RT-)qPCR protocols for each virus (Fig. S4). For all viruses, replication efficiency differed between cultures. qPCR results from samples collected 24 h p.i. at lower and higher MOIs were consistent for PV, RV, HSV, and MV (Fig. S5). For AdV, qPCR was performed with samples collected 3 and 24 h p.i. at MOI 100 to assess viral entry and replication dynamics. AdV genome copies were higher at 24 h p.i. compared to 3 h p.i., indicating permissiveness for AdV. Genome replication of HSV and PV showed several log-fold differences between the cultures, while for RV these differences were not as pronounced. Interestingly, MV gene copies reached similar levels for all but one culture, PC31. MV gene copies in this culture were about one log higher than in the other cultures.

Genome replication correlated to some extent with reduction in cell viability (Figs. S4 and S5). However, for some cultures, e.g., PC06 for PV and RV, PC28 for MV, although showing rather high copy numbers, only a minor reduction in cell viability could be detected. On the other hand, some cultures with rather low copy numbers, e.g., PC03 for MV and PC17 for HSV, showed a major reduction in cell viability upon infection.

As an indicator for virus-mediated cytotoxicity, LDH release was measured (Fig. S4). For PV and RV, and to a lesser extent also for AdV, the release of LDH was in line with the reduction in cell viability (Fig. S4). For MV and HSV, this observation could not be made. In contrast to previously published data for melanoma,[46] PDAC cultures infected with HSV did not release LDH, as shown for eight cultures in Fig. S4.

Quantification of infectious viral progeny production after treatment (Fig. S4) yielded results that correlated in part with the data from the other assays. For RV, higher titers of viral progeny were found in cultures with a higher LDH release upon infection. However, the highest titer of PV progeny was detected in the supernatant from PC18, a culture that showed little cell death and LDH release upon infection with PV. For T-VEC, titers of viral progeny correlated best with the quantification of viral genome expression through qPCR. For all five viruses, high titers of viral progeny were detected in the supernatant of PC31.

Overall, these data illustrate that patient-derived PDAC cultures exhibit individual response patterns to oncolytic virotherapy.

Molecular subtypes of PDAC show differential sensitivity to PV, RV, and HSV

With the aim to identify predictive biomarkers for virotherapy in PDAC, transcriptome profiling of all cultures in an uninfected state was performed using the Clariom S human microarray platform. K-means clustering with 3 subgroups indicated two main transcriptomic clusters, consisting of 6 and 7 cultures each, and one outlier, PC17 (Fig. 3a). We compared the transcriptome-based classification with overall sensitivity to each virus based on cell viability upon infection (Fig. 3b). Remarkably, we found that subgroup 1 seemed overall more sensitive to three of the five OVs compared to the other subgroup. Subgroup 1 was significantly more sensitive to PV, RV, and HSV compared to subgroup 2.

Differential gene expression analysis between subgroup 1 and 2 (Fig. S6a) revealed signature genes associated with previously described molecular subtypes of PDAC, including keratin 6A (KRT6A), tetraspanin 8 (TSPAN), and lysozyme (LYZ).[47–49] Further focus on these signature genes confirmed this association, with subgroup 1 corresponding to the quasi-mesenchymal or basal-like subtype, and subgroup 2 corresponding to the classical subtype as described by Moffitt et al. (Fig. 3c).[47] This stratification is further supported using the signatures described by Collisson et al. and Chan Seng Yue et al. (Fig. S6b and c).[48,49]

Taken together, these findings indicate that the quasi-mesenchymal or basal-like molecular subtype of PDAC may be overall more sensitive to PV, RV, and HSV compared to the classical subtype. Interestingly,

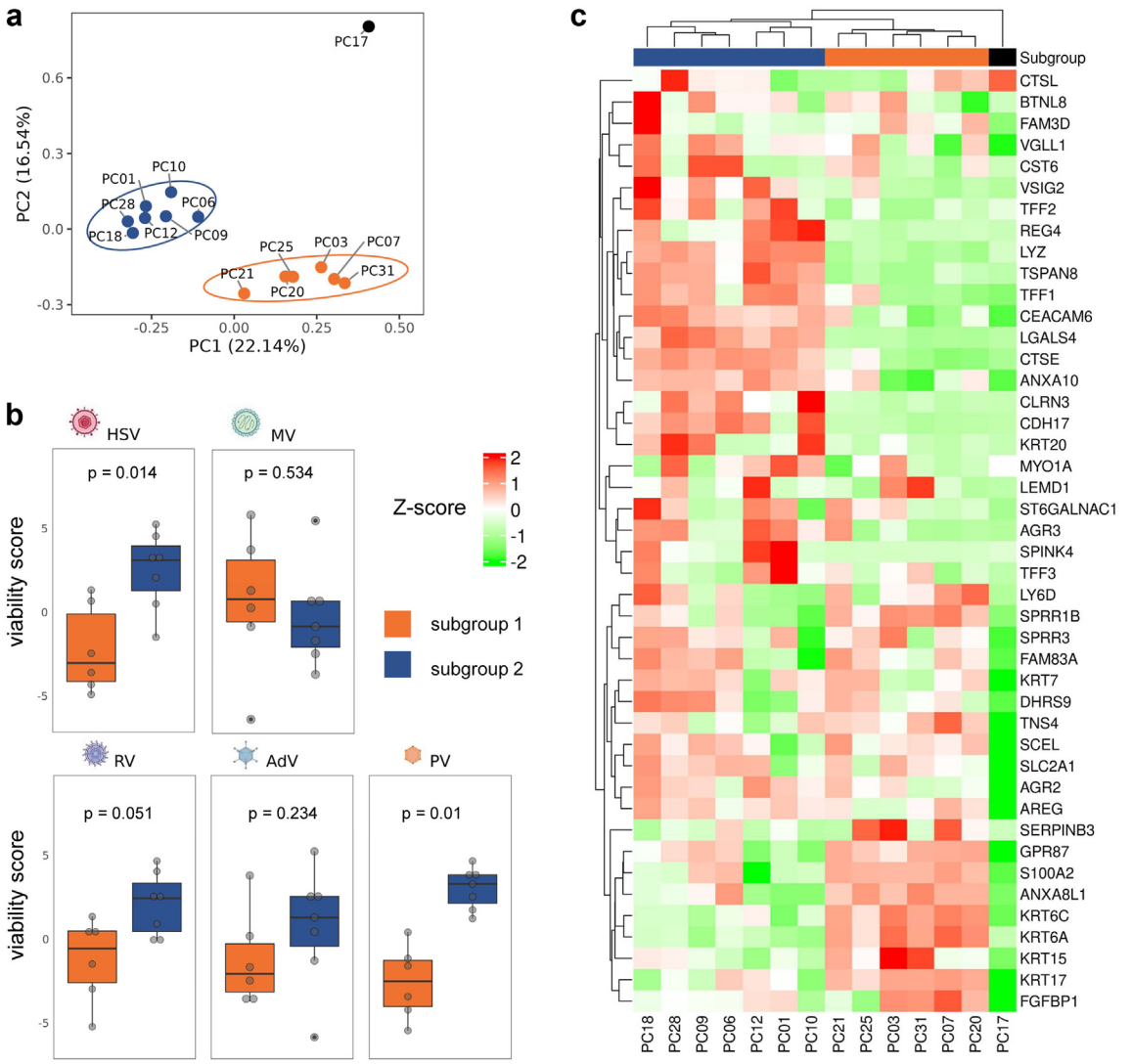

Fig. 3: Molecular subtype of PDAC determines sensitivity to PV, RV, and HSV a. Biplot depicting the first two principal components of the PDAC normalised gene expression matrix. The colors and ellipses represent the subgroups defined by k-means clustering. b. Viability scores per molecular subgroup for each virus, as depicted by boxplots with individual observations. p = 0.014 for HSV, p = 0.534 for MV, p = 0.051 for RV, p = 0.234 for AdV, p = 0.01 for PV (two-sided Wilcoxon rank sum test). c. Heatmap depicting expression of PDAC subtype-defining genes as described by Moffitt et al.,[47] annotated with respective molecular subgroups. See Fig. S6b and c for signatures described in 48 and 49.

sensitivity to MV and AdV did not seem to be associated with PDAC molecular subtype.

With the aim to test this hypothesis in a separate cohort of PDAC cultures, a RT-qPCR panel of 12 subtype-specific marker genes was established to distinguish the subtypes (Fig. S6d). Using this panel, cultures from our initial cohort were clearly identified as belonging to either the basal-like (PC31) and classical (PC01) subtype. In contrast, of four cultures from a separate cohort (PAC1164, PACX34, PACF005, and PACF002) the former three all belonged to the classical subtype, while the latter could not be classified. In support of our findings, the three cultures did not show strong sensitivity to PV, RV, and HSV (data not shown).

When analyzing commonly used PDAC cell lines, BxPc3 and T3M-4 showed a basal-like expression pattern, while HPAC and Capan-I showed an expression pattern corresponding to the classical subtype of PDAC. The majority of tested cell lines (AsPC-I, Panc-I, IMIM-PC2, and MIA PaCa-2) were found not to exhibit expression patterns typical for either of the two subtypes. These findings reinforce the notion that the cohort of 14 patient-derived PDAC cultures employed in this screen more closely represents the molecular

landscape found in primary PDAC than commercially available PDAC cell lines and underlines the importance to establish relevant PDAC model systems.

Biomarker screen retrieves known host factors for individual OVs

We next tested whether our approach retrieved known host cell factors implicated in replication of the five viruses as potential biomarkers for virotherapy by studying the correlation between expression of previously reported host factors and viability scores for specific viruses.

The cellular type I interferon (IFN) response exerts potent antiviral effects. MV vaccine strains used for oncolytic virotherapy are known to be especially IFN-sensitive.[50] Kurokawa et al. previously reported a signature of 22 interferon-stimulated genes (ISGs) associated with relative resistance to MV oncolysis.[51] Overall cell viability was strongly associated with this 22 ISG signature (i.e., high basal expression of ISG and high cell viability) for MV, and to a lesser extent also for RV. Expression of certain ISGs was also associated with viability upon PV and HSV treatment (Fig. 4a). A strong association was observed between MV sensitivity and expression of MX1 (ρ = 0.7407, Fig. 4b). MX1 (Interferon-induced GTP-binding protein Mx1) has been shown to exert anti-viral activity against many RNA and several DNA viruses.[52] For AdV treatment, the correlation seemed to be inverse: Higher expression of some ISGs (OAS2, IFIT1, IFIT3) was associated with a lower cell viability upon infection with AdV (Fig. 4a).

Differential expression of pro- and anti-apoptotic factors may also impact oncolytic virotherapy. For PV, BCL-2 anti-apoptotic proteins have been previously described to limit oncolysis in different solid tumours.[9,10] In support of this, we found that the expression of BCL2L15 was strongly correlated with a higher cell viability upon infection with PV (ρ = 0.7582, Fig. 4b). These results indicate that BCL2L15 may serve as a biomarker for resistance against PV treatment in PDAC. Furthermore, we found that expression of caspase-1 correlated with sensitivity to PV (Fig. 4b). Caspase-1, a promoter of pyroptotic cell death, has been implicated in PV oncolysis of PDAC previously.[53]

Previously, a siRNA library screen for PV host factors as well as a screen of PV susceptibility in 53 cancer cell lines from the NCI-60 panel have been carried out.[54] Overlap analysis between these and the present dataset (Fig. S7) identified 44 common genes in the siRNA screen and 27 common genes in the NCI-60 screen associated with sensitivity to PV. Notably, Galectin-1 (LGALS1), which was described to have a role in PV entry,[55] was the single common factor associated with sensitivity across all three screens (compare Fig. 4b), underlining its importance in the PV replication cycle.

For RV, cathepsins B and L have been identified as secreted factors that support JAM-A-independent infection in glioblastoma spheroids by mimicking endosomal disassembly of the virus.[56] Cathepsins B and L were expressed at similar levels in all PDAC cultures (Supplementary Data 1). Interestingly, in the present study using JAM-A-independent RV, cathepsin E and S expression seemed to inversely correlate with sensitivity to RV (Fig. 4b). Perhaps RV is prematurely processed by cathepsins in these PDAC cultures, hampering oncolytic efficacy.

For HSV, Nectin-1 expression has recently been associated with sensitivity to T-VEC in melanoma.[46] Here, we found a weak correlation between Nectin-1

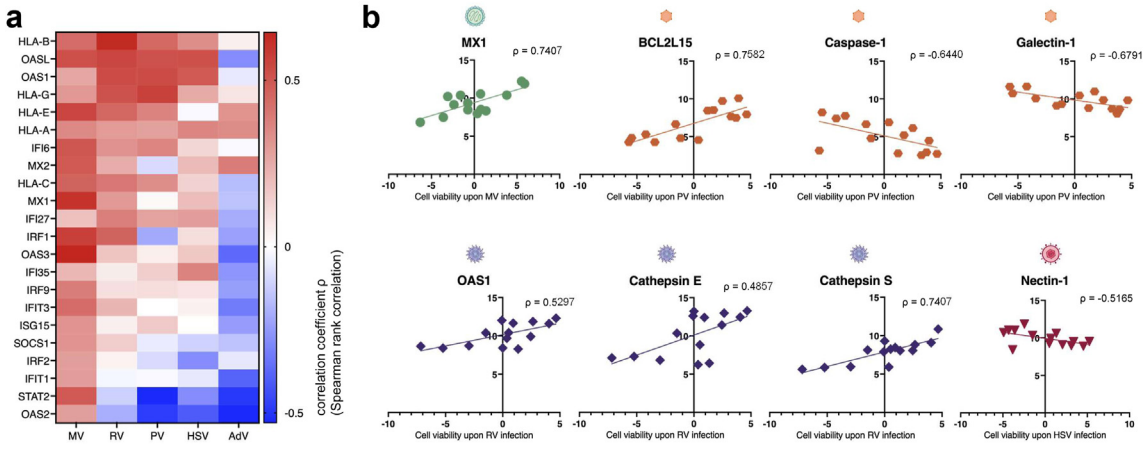

Fig. 4: Biomarker screen retrieves known host factors for individual oncolytic viruses a. Interferon-stimulated genes (ISGs) as restriction factors for MV. Spearman's rank correlation between gene expression of the previously published signature of 22 ISGs affecting MV oncolysis[51] and the viability scores for each OV. b. Host factors for OVs. Spearman's rank correlation of gene expression of selected genes in n = 14 patient-derived cultures with normalised cell viability upon infection with the respective OV.

and T-VEC oncolysis in PDAC cultures (ρ = –0.5165, Fig. 4b).

Post-entry factors rather than expression of viral entry receptors determine outcome of oncolysis in PDAC cultures

We assessed the acquired data for additional correlations between the expression of viral entry receptors and reduction in cell viability (Fig. S8).

For HSV, aside from the weak correlation of oncolysis with Nectin-1 expression, the expression of other HSV-1 (co-)receptors and entry factors described in literature,[57] including HVEM, HSPG2, MAG, MYH9, and PILRa did not correlate with T-VEC oncolysis (data not shown).

To date, the cellular receptor(s) for RV jin-3 have not been determined, but may include sialic acid residues.[11] Ad5 uses coxsackie adenovirus receptor (CAR) as well as integrins αvβ5 and αvβ3 for cell entry.[58] MV vaccine strains use ubiquitous CD46, epithelial Nectin-4, and lymphocytic CD150 as entry receptors.[59] Similar RNA expression levels of these receptors were observed across all cultures (Fig. S8a and b, Supplementary Data 1). RNA expression of CAR was lower in PC17 and flow cytometry confirmed low CAR protein expression in this culture (Fig. S8a). These results suggest that CAR could be a limiting factor for AdV oncolysis in PC17. However, qPCR for AdV genome copies 3 h p.i. did not reveal a lower copy number in PC17 compared to other cultures, which argues against this hypothesis (Fig. S4). Of note, in contrast to RNA microarray data, CAR and CD46 protein expression as detected by flow cytometry fluorescence intensity showed different expression levels across the PDAC cultures (Fig. S8a and b). Flow cytometry data indicated that high CAR protein expression may be associated with increased AdV-mediated oncolysis, with the exception of PC09 (Fig. S8a). Previous research has established that a certain threshold of CD46 expression is required for MV oncolysis.[60] However, neither microarray nor flow cytometry data suggested that CD46 limits MV efficacy in the present set of patient-derived PDAC cultures (Fig. S8b).

PV was recently shown to depend on the expression of Laminin C1 (LAMC1) and Galectin-1 (LGALS1) for cell entry.[55] Despite similar expression levels across all cultures, there was a weak correlation of reduction in cell viability with higher expression of Galectin-1, as shown in Fig. 4b. These results suggest that expression of Laminin C1 is not a limiting factor for PV oncolysis in this context, but support the role of Galectin-1 in PV oncolysis.

In the AdV used in this study, E1 expression is controlled by the human telomerase (hTERT) promoter. We therefore checked expression of telomerase (TERT) in the PDAC cultures. Of note, TERT expression levels were similar across all cultures with the exception of PC17 (Fig. S8c), suggesting that this is not a major determinant of AdV (Ad5-hTERT) sensitivity in these PDAC cultures. Thus, additional cellular factors could account for response or resistance to these OVs.

Cellular pathways associated with sensitivity to virotherapy

Overall, these data suggest that post-entry factors rather than expression of viral entry receptors determine outcome of virotherapy in PDAC. We therefore pursued an unbiased approach to identify candidate biomarkers for virotherapy of PDAC and searched for correlations with cell viability upon OV treatment for each virus separately (Supplementary Data 2).

To this end, we performed Gene Set Enrichment Analysis[35] using the Spearman correlation between gene expression and cell viability score for each virus using the Molecular Signatures Database HALLMARK gene set collection.[37] Enriched HALLMARK pathway process categories suggested that activation of immunological pathways was associated with resistance to MV, and also to RV and PV, albeit to a lesser extent (Fig. 5). Cell proliferation pathways were generally associated with response to virotherapy. Certain metabolic and signaling pathways seemed to be associated with response, others with resistance to virotherapy (Fig. 5 and Fig. S9). Specifically, pathway analyses revealed that IFN signaling, TNFα signaling via NF-κB, and IL6 JAK/STAT signaling may confer relative resistance to MV, RV, PV, and HSV treatment. Proliferative signaling involving E2F targets and the G2M checkpoint may be associated with response to PV, RV, and MV. For PV, E2F activity is a known requirement for early p4 promoter activation.[61] Interestingly, epithelial to mesenchymal transition seemed to be associated with relative resistance to AdV and MV, but with sensitivity to HSV. PI3K-AKT and Wnt/β-Catenin signaling as well as oxidative phosphorylation appeared to be correlated with responsiveness to AdV, HSV, and PV. Xenobiotic metabolism was identified to potentially inhibit oncolysis. Tumours characterised by hypoxia and p53 activation may be responsive to HSV and AdV, but not to MV and RV. Of note, there was no overt association of KRAS status of PDAC cultures (Fig. 1b) with sensitivity to virotherapy (compare also Fig. 2c).

These results emphasise the differing response patterns of the patient-derived PDAC cultures to the five different OVs.

MV plus cGAS inhibition as a potential combination therapy in selected PDAC

Another approach to biomarker identification is the analysis of exceptional responders. One PDAC culture, PC31, showed exceptional sensitivity to MV oncolysis. Transcriptome analysis showed that HIST1H2AE and MB21D1 (which encodes cyclic GMP-AMP synthase, cGAS) are expressed at low levels in PC31 compared to

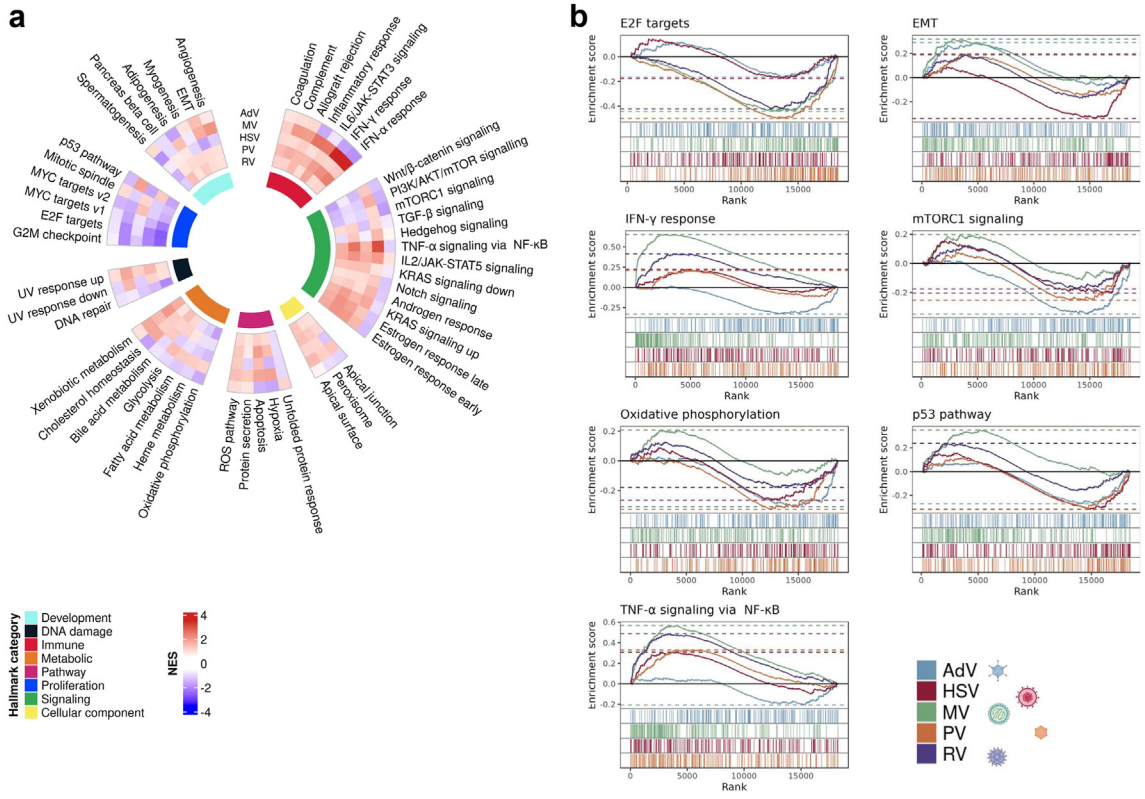

Fig. 5: Gene set enrichment analysis a. Circular heatmap depicting normalised enrichment scores (NES) for HALLMARK pathways and corresponding process categories (as described in 37) based on viability scores for each OV. OVs hierarchically clustered. A higher NES score indicates many genes in the respective HALLMARK gene set are positively correlated with the viability score for that OV. b. Plots depicting running ES and rank for genes in depicted HALLMARK gene set for each OV. See Supplementary Data 2 for respective leading edge genes.

all other PDAC cultures. We thus hypothesised that cGAS may restrict MV replication. To test this hypothesis, we combined MV treatment with the cGAS inhibitor G140 in four other PDAC cultures (Fig. 6). Baseline expression levels of cGAS were equally high in these three cultures as compared to PC31 (Fig. 6a). Interestingly, the combination showed improved efficacy in two of the three cultures (Fig. 6b). Two PDAC cell line (T3M-4 and MIA PaCa2-) and PC31 derivatives overexpressing human cGAS were generated by lentiviral transduction. Cells transduced with a vector encoding RFP served as controls (Supplementary Methods, Fig. S10). Monitoring of the infection kinetics of PC31-cGAS and the control culture PC31-RFP with MV-GFP using the IncuCyte system (Fig. 6c, Supplementary videos 1 and 2) revealed a delayed onset of syncytia formation and GFP expression in the culture overexpressing cGAS compared to PC31-RFP. Cell viability 72 h p.i (Fig. 6d) was markedly higher in PC31-cGAS, and a crystal violet stain 7 days p.i. showed higher cell abundance in PC31-cGAS (Fig. 6e). The effect was most pronounced for lower MOIs of MV, i.e., 0.03 and 0.1. Release of infectious viral progeny 72 h post infection was quantified by titration and found to be lower in the culture overexpressing cGAS (Fig. 6f). Despite lower fold-change levels in T3M-4 and MIA PaCa-2 cell lines, overexpression of cGAS also rendered these cells less sensitive to MV (Fig. S10c). Taken together, these results indicate that cGAS may contribute to MV unresponsiveness in some PDAC tumours, which could be overcome by higher dose levels and/or by co-administration of cGAS inhibitors.

Discussion

Oncolytic virotherapy (OVT) is an emerging treatment option for a range of tumour entities including PDAC, as highlighted by the number of ongoing clinical trials (Table S1). We observed that surgical explants of PDAC are susceptible to infection with five clinically relevant OVs, albeit to different extents and exhibiting differing response patterns.

Using patient-derived cultures, this study shows that OVT is a viable treatment option for this tumour entity, as the majority (12/14) of heterogenous patient-derived PDAC cultures were responsive to at least one of five

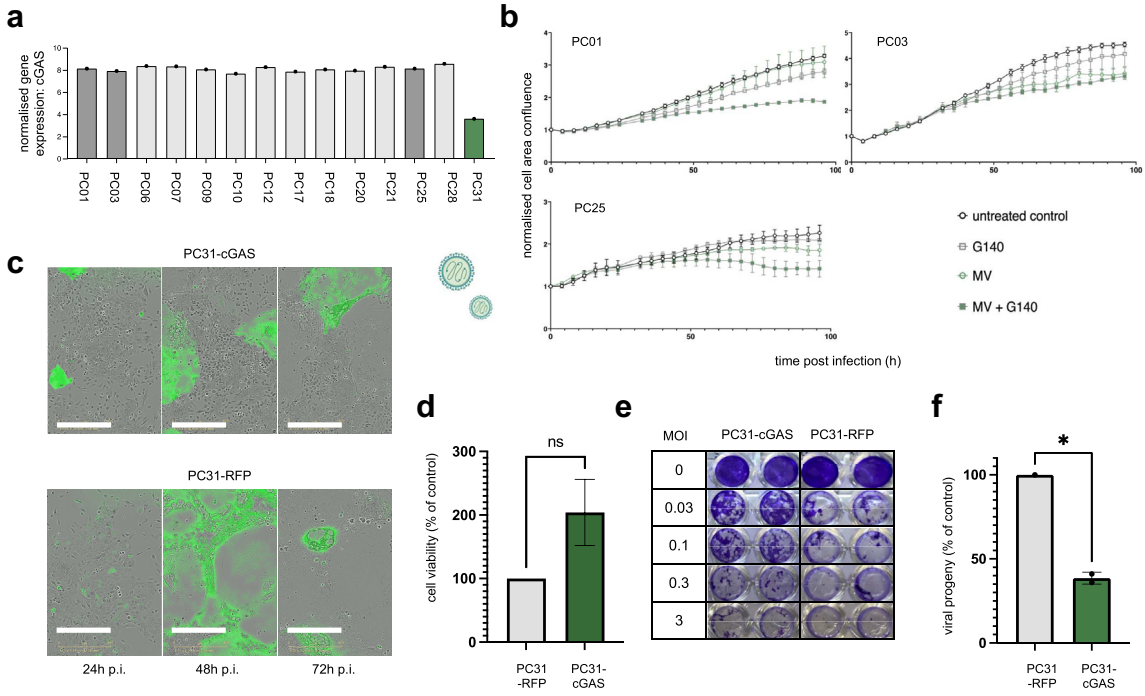

Fig. 6: MV plus cGAS inhibition combination therapy a. Relative cGAS expression in n = 14 patient-derived PDAC cultures. Bar graph depicting normalised gene expression for cGAS in all PDAC cultures as determined in RNA microarray. Cultures used in b are depicted in dark grey, PC31 (exceptional responder to MV) is highlighted in green. b. Live cell analysis after MV and cGAS inhibitor treatment. PDAC cultures PC01, PC03, and PC25 were seeded in 96-well plates in technical duplicates. After 24 h, cultures were either subjected to mock infection or treated with MV (PC01 and PC03 MOI 0.3; PC25: MOI 3) and/or the cGAS inhibitor G140 (10 µm). Live cell analysis was performed using the IncuCyte instrument and normalised cell area confluency was automatically calculated based on time point of infection. Time course over 100 h p.i. is shown. Mean values of duplicates and standard deviation are plotted. c. PC31-cGAS and PC31-RFP were seeded in 96-well cell culture plates and infected with MV-GFP (MOI 0.1) and monitored in the IncuCyte instrument over three days (scale bars 400 µm). d. PC31-cGAS and PC31-RFP were seeded in 96-well cell culture plates in duplicates and infected with MV-GFP (MOI 0.3), viability was assessed 72 h post infection. Viability of PC31-RFP was defined as 100%. For PC31-cGAS, mean value and standard deviation from n = 3 independent experiments are shown; p = 0.2254 (unpaired t-test). e. PC31-cGAS and PC31-RFP were seeded in 96-well cell culture plates and infected with MV-GFP (MOIs 0.03, 0.1, 0.3, and 3) or subjected to mock infection in duplicates. Seven days post infection, viable cells were stained using crystal violet. f. PC31-cGAS and PC31-RFP were seeded in 96-well cell culture plates and infected with MV-GFP (MOI 0.3). 72 h post infection, supernatant was harvested and viral progeny was quantified by endpoint dilution assay on Vero cells in octuplicates. Mean and standard deviation from n = 2 independent experiments are shown; p = 0.0447 (unpaired t-test).

clinically relevant OVs. However, we observed a broad spectrum of responses, with no single agent being suitable for all PDAC cultures. These findings underline the importance of pre-treatment patient stratification for eligibility for OVT and for choice of OV in the frame of personalised cancer treatment.

Cross-resistances between OVT and radiation, chemotherapy, or targeted therapy are presumably uncommon,[62] indicating that OVs target different vulnerabilities of malignant cells compared to established treatment modalities. Our data show that each OV in turn addresses specific subsets of PDAC cultures.

One of the strongest correlations we observed was between baseline ISG expression of PDAC cultures and relative resistance to MV, as reported previously for patient-derived glioblastoma cultures and sarcoma cell lines.[51,63] In contrast, PV and HSV have been characterised as insensitive to IFN in PDAC.[64,65] However, our study suggests that, although to a lesser extent than MV, these two viruses may also be restricted by ISGs in PDAC. Our results imply that AdV may be the most suitable OV for PDAC with high baseline ISG expression, whereas PDAC with defects in IFN signaling may be especially sensitive to MV. Many viruses including HSV and AdV counteract the cellular IFN response.[66] A previous study has suggested that an aggressive form of PDAC characterised by a cell-intrinsic IFN signature could be targeted by agents that block this pathway,[67] highlighting the potential of OVT in PDAC.

In this study, one representative virus from five families was chosen to reflect the current clinical landscape of OVT in PDAC. These five OVs harbor specific genetic modifications which may impact oncolytic

efficacy; other representatives of these virus families may show different efficacy profiles, e.g., due to altered replicative capacity. While strictly all conclusions from the present data set must constrain to the specific OVs studied, factors relating to the inherent biology of a certain virus family will be transferable to related OVs. Of note, additional AdV and MV derivatives are in development, and teserpaturev/G47Δ, an HSV-1 with deletions in the *α47* and *γ34.5* genes as well as the *US11* promoter, recently received conditional, limited approval in Japan for treatment of glioblastoma.[68–70] In case of reovirus, mainly Pelareorep (Reolysin), an unmodified isolate, is applied. We opted for the reovirus jin-3 variant with broader tropism to reveal receptor-independent tumour cell factors. Our results for the other viruses indicate that also post-entry factors rather than receptor expression alone determine response to OVT.

In the present dataset, few entry factors were associated with OV efficacy: Higher RNA expression of Galectin-1, which plays an important role in PV entry,[55] correlated with PV oncolytic activity. CAR protein levels partially correlated with AdV efficacy. However, one culture (PC09) responded exceptionally well to AdV, although expression of CAR as detected by flow cytometry was rather low.

Direct comparison of post-entry phenomena for the different OVs is challenging, as they differ vastly in terms of their biological properties and replication cycle. Virus dosing and assay time points were adjusted to account for these differences, limiting direct comparability of the assay results between different OVs. The quality of virus preparations may additionally affect assay results. Clinical-grade virus stocks were available for two of the five OVs, while three viruses were obtained as preclinical research grade preparations. Nevertheless, recovery of known host factors for individual viruses indicates that our approach is suitable to identify veritable determinants of OVT efficacy.

While several previously characterised factors were retrieved, we also noted differences to previous reports on potential OVT biomarkers. One study has reported genes upregulated in AdV-resistant human ovarian cancer cell line clones after in vivo selection.[71] In contrast to our results, that study identified IFN signaling as an AdV resistance factor. Both IFNα and –γ have been shown to restrict AdV replication, thereby promoting viral persistence, in benign primary human cells but not in cancer cell lines.[72,73] A recent study showed that Nectin-1 receptor expression correlates with sensitivity of human melanoma to T-VEC,[46] while our data indicate a weak correlation in PDAC. These findings indicate that at least some biomarkers for OVT may be specific for a certain tumour entity.

In PDAC, the molecular subtype of a given tumour may serve as a primary indicator for patient stratification in OVT: The quasi-mesenchymal subtype of PDAC seems more amenable to PV, RV, and HSV treatment. Remarkably, this is the PDAC subtype with worse prognosis.[47] In a recent Phase II clinical trial of PV in PDAC, clinical responses were observed in two of seven patients.[74] No predictive biomarker candidates were investigated in this study and PDAC molecular subtypes were not reported, but responding patients showed possible immunological correlates of efficacy, i.e., an increase in intratumoural T cell infiltration and an increase in serum levels of pro-inflammatory cytokines and IFN. Ultimately, all biomarkers and potential combination treatments will require validation in a clinical setting.

The present in vitro study aimed at identifying tumour cell-intrinsic vulnerabilities to OVs and did not assess effects within the tumour microenvironment and especially immunological effects of OVT, which have recently come into focus. Viral replication and virus-induced cell death elicit pathogen- and danger-associated molecular patterns (PAMPs and DAMPs) and concomitant release of tumour antigens, resulting in tumour vaccination effects.[75] Thus, OV replication and cell killing are considered prerequisites for immunotherapeutic efficacy of OVT.[76] Distinct OVs may induce different modes of cell death. Interestingly, PDAC cultures released LDH upon treatment with four OVs, but not after treatment with HSV. Release of intracellular material may increase local inflammation and immunogenicity. Previous studies have demonstrated induction of immunogenic cell death (ICD) in PDAC by AdV serotype 5, H-1PV, HSV-1, and MV.[53,77–80] For RV jin-3, hallmarks of ICD were found after treatment of patient-derived prostate cancer models.[81]

In any case, OVT should aim at initial induction of immunogenic cell death via effective tumour cell lysis. In this regard, combination treatments are one strategy to enhance efficacy. Accordingly, combination of MV with JAK inhibitors has been applied preclinically to counteract IFN-mediated resistance to MV.[51] However, as IFN sensitivity is a central hallmark of MV attenuation,[50] this combination may elicit safety concerns. Interestingly, we found that cGAS downregulation was associated with an exceptional response to MV in one patient-derived culture; overexpression of cGAS in this culture and in two PDAC cell lines rendered the cells less sensitive towards MV. Though known as a canonical DNA sensor, recent studies have implicated cGAS in sensing of fusogenic viruses and paramyxoviruses including measles virus.[82–84] In the present study, a cGAS inhibitor enhanced MV efficacy in some PDAC cultures, supporting this combination strategy. In contrast, agonists of the cGAS/STING pathway are investigated as cancer immunotherapeutics (NCT02675439, NCT03010176, NCT04144140). However, cGAS/STING may also promote tumour growth and immunosuppression,[85] indicating that MV plus cGAS inhibition may be suitable only in certain settings.

Overall, rational design of combination regimens will be key to devise successful OV-based therapies.[86] Many current clinical trials in PDAC investigate OVs in combination with chemo- or immunotherapy (Table S1). Nevertheless, different responses to the combination of MV and cGAS inhibitor again underscore that tumour cell factors facilitating or limiting OVT are most likely patient-specific.

In conclusion, the present study reports the broad spectrum of OVT responses in patient-derived PDAC cultures. Individual response patterns were observed, likely reflecting tumour heterogeneity. Correlative analyses showed that PDAC molecular subtype, ISG expression and activation of distinct signaling and metabolic pathways may guide initial patient stratification in OVT. However, no single gene or pathway fully explains the spectrum of response patterns observed for individual OVs. Complex biological therapies such as OVT most likely do not depend on single-gene biomarkers. Further dissecting patterns of sensitivity and resistance, including commonalities and divergences between viruses and patient samples can help unravel the multifaceted mechanisms underlying efficacy of OVT. By providing all primary data, this study provides a rich source for discovery of additional associations. Given the inter-individual differences in response, prospective functional stratification by ex vivo sensitivity analysis on patient-derived biopsy material and/or short-term cultures may be required to assess eligibility for OVT (Fig. S1b). While more elaborate techniques such as single-cell sequencing and proteomics are being developed, we opted for transcriptome analysis by RNA microarray for biomarker discovery. In contrast to other techniques, transcriptome analysis is readily available at fairly low cost and thus may be most broadly applicable in a clinical setting.

Future endeavors with larger datasets may further refine pre-treatment biomarkers for OVT. As one noteworthy initiative, the Dutch Oncolytic Viro-ImmunoTherapy (OVIT) envisions comparison of several OVs in near-patient models of several tumour entities.[87] In particular, correlative research programs searching for predictive biomarkers within OVT clinical trials will be key to promote application of OVT for the benefit of patients afflicted with cancer.

Contributors

Study concept and design: C.E.E., T.E.S., L.I.K., C.R.B.; Development of methodology: Z.M., T.E.S., F.V.H., J.A., C.R.B., P.S.; Acquisition, analysis and interpretation of data, statistical analysis: T.E.S., L.I.K., F.V.H., A.H., S.C.S.P., A.J., M.S.C.F., B.S., S.A., A.K., K.S., W.Z., S.T.F.B., V.K., M.A., H.M.K., A.R.P.; Resources: L.J.A.C.H., A.E., A.M., R.C.H., S.H., J.D., F.G., G.U.; T.E.S., L.I.K., F.V.H., C.R.B., and C.E.E. verified the underlying data. T.E.S., L.I. K., and C.E.E. wrote the manuscript. All authors read and approved the final manuscript.

Data sharing statement

Availability of data and materials: Gene expression data and z-score normalised experimental data are available as Supplementary Data. Microarray data of the 14 patient-derived cultures is available via the European Genome-Phenome Archive (EGA) at https://ega-archive.org/studies/EGAS00001007001. Additional data and materials can be made available upon request.

Declaration of interests

A.M. is inventor on several PV-related patents and patent applications. G.U. acts as CMO, CSO, and COO of CanVirex, a company developing oncolytic viruses for cancer therapy. C.E.E. is listed as inventor on patent applications filed by her institution related to the development of RNA viruses for cancer immunotherapy. S.H. reports an advisory role and honoraria from Amgen. L.J.A.C.H. received a grant from Flanders Innovation & Entrepreneurship (HBC18-2002) for the development of a PDXO drug screening platform.

Acknowledgements

We thank the Microarray Unit of the Genomics and Proteomics Core Facility, German Cancer Research Center (DKFZ), for providing excellent Expression Profiling services. We are grateful to Linda Küther, Anette Rohrhofer, Tim Kindinger, Stefanie Sawall, Jessica Albert, Birgit Hoyler, and Stefanus G.T. Janson for technical assistance as well as to Oliver Heil, J. Ole Klarhof, Alessia Floerchinger, Na Kang, and Nadine van Montfoort for helpful discussions. We are grateful to Barbara Leuchs for providing H-1PV. We thank Mieke Mertens and Daniel Seebach-Schielzeth, University Hospital Heidelberg Pharmacy, for assistance in acquiring T-VEC. We are grateful to Gemma Pidelaserra Martí, Jonny Hertzog, and Johannes P. W. Heidbuechel for comments on the manuscript.

Fig. S1 and virus icons in the figures were created using Biorender.com.

Funding: This work was supported by the German National Science Foundation (Deutsche Forschungsgemeinschaft, DFG EN 1119/2-2, to C.E.E.). T.E.S. received a Mildred Scheel Fellowship provided by the German Cancer Aid (Deutsche Krebshilfe). M.S.C.F. is supported by a doctoral scholarship of the German National Academic Scholarship Foundation (Studienstiftung des deutschen Volkes). S.T.F.B. was funded by the Survival with Pancreatic Cancer Foundation, Utrecht, Netherlands (AOK_LUMC-2017-2). V.K. was supported by a personal grant from the Dutch Research Council (NWO-talent program Veni, ZonMW), as well as funding from the Dutch Foundation "Overleven met Alvleesklierkanker" (SOAK 21.02). L.J.A.C.H. received funding from Flanders Innovation and Entrepreneurship (HBC18-2002). A.R.P. received support from the Mildred Scheel Early Career Center Dresden P2, funded by the German Cancer Aid. The funders were not involved in the design of the study or collection, analysis, or interpretation of data or in writing the manuscript.

Appendix A. Supplementary data

Supplementary data related to this article can be found at https://doi.org/10.1016/j.ebiom.2024.105219.

References

1 Mizrahi JD, Surana R, Valle JW, Shroff RT. Pancreatic cancer. *Lancet*. 2020;395(10242):2008–2020.
2 Marchini A, Daeffler L, Pozdeev VI, Angelova A, Rommelaere J. Immune conversion of tumor microenvironment by oncolytic viruses: the protoparvovirus H-1PV case study. *Front Immunol*. 2019;10:1848.
3 Macedo N, Miller DM, Haq R, Kaufman HL. Clinical landscape of oncolytic virus research in 2020. *J Immunother Cancer*. 2020;8(2):e001486.
4 Marchini A, Ilkow CS, Melcher A. Oncolytic virus immunotherapy. *Cancers (Basel)*. 2021;13(15).
5 Lanson NA JR, Friedlander PL, Schwarzenberger P, Kolls JK, Wang G. Replication of an adenoviral vector controlled by the human telomerase reverse transcriptase promoter causes tumor-selective tumor lysis. *Cancer Res*. 2003;63(22):7936–7941.
6 Duprex WP, McQuaid S, Hangartner L, Billeter MA, Rima BK. Observation of measles virus cell-to-cell spread in astrocytoma cells

by using a green fluorescent protein-expressing recombinant virus. *J Virol*. 1999;73(11):9568–9575.
7 Veinalde R, Grossardt C, Hartmann L, et al. Oncolytic measles virus encoding interleukin-12 mediates potent antitumor effects through T cell activation. *Oncoimmunology*. 2017;6(4):e1285992.
8 Dingli D, Peng K-W, Harvey ME, et al. Image-guided radiovirotherapy for multiple myeloma using a recombinant measles virus expressing the thyroidal sodium iodide symporter. *Blood*. 2004;103(5):1641–1646.
9 Bretscher C, Marchini A. H-1 parvovirus as a cancer-killing agent: past, present, and future. *Viruses*. 2019;11(6):562.
10 Hartley A, Kavishwar G, Salvato I, Marchini A. A roadmap for the success of oncolytic parvovirus-based anticancer therapies. *Annu Rev Virol*. 2020;7(1):537–557.
11 van den Wollenberg DJ, Dautzenberg IJC, van den Hengel SK, et al. Isolation of reovirus T3D mutants capable of infecting human tumor cells independent of junction adhesion molecule-A. *PLoS One*. 2012;7(10):e48064.
12 Ferrucci PF, Pala L, Conforti F, Cocorocchio E. Talimogene laherparepvec (T-VEC): an intralesional cancer immunotherapy for advanced melanoma. *Cancers (Basel)*. 2021;13(6):1383.
13 Ehrenberg KR, Gao J, Oppel F, et al. Systematic generation of patient-derived tumor models in pancreatic cancer. *Cells*. 2019;8(2):142.
14 Boozari B, Mundt B, Woller N, et al. Antitumoural immunity by virus-mediated immunogenic apoptosis inhibits metastatic growth of hepatocellular carcinoma. *Gut*. 2010;59(10):1416–1426.
15 Gao J, Zhang W, Mese K, Bunz O, Lu F, Ehrhardt A. Transient chimeric ad5/37 fiber enhances NK-92 carrier cell-mediated delivery of oncolytic adenovirus type 5 to tumor cells. *Mol Ther Methods Clin Dev*. 2020;18:376–389.
16 Heidbuechel JPW, Engeland CE. Paramyxoviruses for tumor-targeted immunomodulation: design and evaluation ex vivo. *J Vis Exp*. 2019;143.
17 Leuchs B, Roscher M, Müller M, Kürschner K, Rommelaere J. Standardized large-scale H-1PV production process with efficient quality and quantity monitoring. *J Virol Methods*. 2016;229:48–59.
18 El-Andaloussi N, Endele M, Leuchs B, et al. Novel adenovirus-based helper system to support production of recombinant parvovirus. *Cancer Gene Ther*. 2011;18(4):240–249.
19 El-Andaloussi N, Leuchs B, Bonifati S, Rommelaere J, Marchini A. Efficient recombinant parvovirus production with the help of adenovirus-derived systems. *J Vis Exp*. 2012;62:3518.
20 Allaume X, El-Andaloussi N, Leuchs B, et al. Retargeting of rat parvovirus H-1PV to cancer cells through genetic engineering of the viral capsid. *J Virol*. 2012;86(7):3452–3465.
21 Grosche L, Döhner K, Düthorn A, Hickford-Martinez A, Steinkasserer A, Sodeik B. Herpes simplex virus type 1 propagation, titration and single-step growth curves. *Bio Protoc*. 2019;9(23):e3441.
22 Schmitt M, Pawlita M. High-throughput detection and multiplex identification of cell contaminations. *Nucleic Acids Res*. 2009;37(18):e119.
23 Castro F, Dirks WG, Fähnrich S, Hotz-Wagenblatt A, Pawlita M, Schmitt M. High-throughput SNP-based authentication of human cell lines. *Int J Cancer*. 2013;132(2):308–314.
24 Harryvan TJ, Hawinkels LJAC, Östman A, Ten Dijke P, Strell C, Hornsveld M. A novel pancreatic cancer mini-tumor model to study desmoplasia and myofibroblastic cancer-associated fibroblast differentiation. *Gastro Hep Adv*. 2022;1(4):678–681.
25 Fallaux FJ, Kranenburg O, Cramer SJ, et al. Characterization of 911: a new helper cell line for the titration and propagation of early region 1-deleted adenoviral vectors. *Hum Gene Ther*. 1996;7(2):215–222.
26 Tattersall P, Bratton J. Reciprocal productive and restrictive virus-cell interactions of immunosuppressive and prototype strains of minute virus of mice. *J Virol*. 1983;46(3):944–955.
27 Dirks WG, MacLeod RAF, Nakamura Y, et al. Cell line cross-contamination initiative: an interactive reference database of STR profiles covering common cancer cell lines. *Int J Cancer*. 2010;126(1):303–304.
28 Robin T, Capes-Davis A, Bairoch A. CLASTR: the Cellosaurus STR similarity search tool - a precious help for cell line authentication. *Int J Cancer*. 2020;146(5):1299–1306.
29 Kemp V, van den Wollenberg DJM, et al. Arming oncolytic reovirus with GM-CSF gene to enhance immunity. *Cancer Gene Ther*. 2019;26(9-10):268–281.
30 Danthi P, Holm GH, Stehle T, Dermody TS. Reovirus receptors, cell entry, and proapoptotic signaling. *Adv Exp Med Biol*. 2013;790:42–71.
31 Lei C, Yang J, Hu J, Sun X. On the calculation of TCID(50) for quantitation of virus infectivity. *Virol Sin*. 2021;36(1):141–144.
32 Gautier L, Cope L, Bolstad BM, Irizarry RA. affy–analysis of Affymetrix GeneChip data at the probe level. *Bioinformatics*. 2004;20(3):307–315.
33 Ritchie ME, Phipson B, Wu D, et al. Limma powers differential expression analyses for RNA-sequencing and microarray studies. *Nucleic Acids Res*. 2015;43(7):e47.
34 Phipson B, Lee S, Majewski IJ, Alexander WS, Smyth GK. Robust hyperparameter estimation protects against hypervariable genes and improves power to detect differential expression. *Ann Appl Stat*. 2016;10(2):946.
35 Subramanian A, Tamayo P, Mootha VK, et al. Gene set enrichment analysis: a knowledge-based approach for interpreting genome-wide expression profiles. *Proc Natl Acad Sci U S A*. 2005;102(43):15545–15550.
36 Korotkevich G, Sukhov V, Budin N, Shpak B, Artyomov MN, Sergushichev A. *Fast gene set enrichment analysis*. 2021.
37 Liberzon A, Birger C, Thorvaldsdóttir H, Ghandi M, Mesirov JP, Tamayo P. The molecular signatures database (MSigDB) hallmark gene set collection. *Cell Syst*. 2015;1(6):417–425.
38 Gu Z, Eils R, Schlesner M. Complex heatmaps reveal patterns and correlations in multidimensional genomic data. *Bioinformatics*. 2016;32(18):2847–2849.
39 Gu Z. Complex heatmap visualization. *Imeta*. 2022;1(3):e43.
40 Gu Z, Gu L, Eils R, Schlesner M, Brors B. Circlize Implements and enhances circular visualization in R. *Bioinformatics*. 2014;30(19):2811–2812.
41 Wickham H. *Data analysis*. Springer; 2016.
42 Oliveros JC. *VENNY. An interactive tool for comparing lists with venn diagrams*, 2007. 2015.
43 De Munck J, Binks A, McNeish IA, Aerts JL. Oncolytic virus-induced cell death and immunity: a match made in heaven? *J Leukoc Biol*. 2017;102(3):631–643.
44 Zeng S, Pöttler M, Lan B, Grützmann R, Pilarsky C, Yang H. Chemoresistance in pancreatic cancer. *Int J Mol Sci*. 2019;20(18):4504.
45 Raghavan S, Winter PS, Navia AW, et al. Microenvironment drives cell state, plasticity, and drug response in pancreatic cancer. *Cell*. 2021;184(25):6119–6137.e26.
46 Schwertner B, Lindner G, Toledo Stauner C, et al. Nectin-1 expression correlates with the susceptibility of malignant melanoma to oncolytic herpes simplex virus in vitro and in vivo. *Cancers (Basel)*. 2021;13(12):3058.
47 Moffitt RA, Marayati R, Flate EL, et al. Virtual microdissection identifies distinct tumor- and stroma-specific subtypes of pancreatic ductal adenocarcinoma. *Nat Genet*. 2015;47(10):1168–1178.
48 Collisson EA, Sadanandam A, Olson P, et al. Subtypes of pancreatic ductal adenocarcinoma and their differing responses to therapy. *Nat Med*. 2011;17(4):500–503.
49 Chan-Seng-Yue M, Kim JC, Wilson GW, et al. Transcription phenotypes of pancreatic cancer are driven by genomic events during tumor evolution. *Nat Genet*. 2020;52(2):231–240.
50 Fontana JM, Bankamp B, Bellini WJ, Rota PA. Regulation of interferon signaling by the C and V proteins from attenuated and wild-type strains of measles virus. *Virology*. 2008;374(1):71–81.
51 Kurokawa C, Iankov ID, Anderson SK, et al. Constitutive interferon pathway activation in tumors as an efficacy determinant following oncolytic virotherapy. *J Natl Cancer Inst*. 2018;110(10):1123–1132.
52 Haller O, Staeheli P, Schwemmle M, Kochs G. Mx GTPases: dynamin-like antiviral machines of innate immunity. *Trends Microbiol*. 2015;23(3):154–163.
53 Angelova AL, Grekova SP, Heller A, et al. Complementary induction of immunogenic cell death by oncolytic parvovirus H-1PV and gemcitabine in pancreatic cancer. *J Virol*. 2014;88(10):5263–5276.
54 Kulkarni A, Ferreira T, Bretscher C, et al. Oncolytic H-1 parvovirus binds to sialic acid on laminins for cell attachment and entry. *Nat Commun*. 2021;12(1):3834.
55 Ferreira T, Kulkarni A, Bretscher C, et al. Oncolytic H-1 parvovirus hijacks galectin-1 to enter cancer cells. *Viruses*. 2022;14(5):1018.
56 Dautzenberg IJC, van den Wollenberg DJM, van den Hengel SK, et al. Mammalian orthoreovirus T3D infects U-118 MG cell spheroids independent of junction adhesion molecule-A. *Gene Ther*. 2014;21(6):609–617.

57 Jayawardena N, Burga LN, Poirier JT, Bostina M. Virus-receptor interactions: structural insights for oncolytic virus development. *Oncolytic Virother*. 2019;8:39–56.
58 Zhang Y, Bergelson JM. Adenovirus receptors. *J Virol*. 2005;79(19):12125–12131.
59 Lin L-T, Richardson CD. The host cell receptors for measles virus and their interaction with the viral hemagglutinin (H) protein. *Viruses*. 2016;8(9):250.
60 Anderson BD, Nakamura T, Russell SJ, Peng K-W. High CD46 receptor density determines preferential killing of tumor cells by oncolytic measles virus. *Cancer Res*. 2004;64(14):4919–4926.
61 Deleu L, Pujol A, Faisst S, Rommelaere J. Activation of promoter P4 of the autonomous parvovirus minute virus of mice at early S phase is required for productive infection. *J Virol*. 1999;73(5):3877–3885.
62 Vile R, Ando D, Kirn D. The oncolytic virotherapy treatment platform for cancer: unique biological and biosafety points to consider. *Cancer Gene Ther*. 2002;9(12):1062–1067.
63 Berchtold S, Lampe J, Weiland T, et al. Innate immune defense defines susceptibility of sarcoma cells to measles vaccine virus-based oncolysis. *J Virol*. 2013;87(6):3484–3501.
64 Neulinger-Muñoz M, Schaack D, Grekova SP, et al. Human retrotransposons and the global shutdown of homeostatic innate immunity by oncolytic parvovirus H-1PV in pancreatic cancer. *Viruses*. 2021;13(6):1019.
65 Moerdyk-Schauwecker M, Shah NR, Murphy AM, Hastie E, Mukherjee P, Grdzelishvili VZ. Resistance of pancreatic cancer cells to oncolytic vesicular stomatitis virus: role of type I interferon signaling. *Virology*. 2013;436(1):221–234.
66 Sohn S-Y, Hearing P. Adenoviral strategies to overcome innate cellular responses to infection. *FEBS Lett*. 2019;593(24):3484–3495.
67 Espinet E, Gu Z, Imbusch CD, et al. Aggressive PDACs show hypomethylation of repetitive elements and the execution of an intrinsic IFN program linked to a ductal cell of origin. *Cancer Discov*. 2021;11(3):638–659.
68 Peter M, Kühnel F. Oncolytic adenovirus in cancer immunotherapy. *Cancers (Basel)*. 2020;12(11):3354.
69 Engeland CE, Ungerechts G. Measles virus as an oncolytic immunotherapy. *Cancers (Basel)*. 2021;13(3):544.
70 Todo T, Ito H, Ino Y, et al. Intratumoral oncolytic herpes virus G47Δ for residual or recurrent glioblastoma: a phase 2 trial. *Nat Med*. 2022;28(8):1630–1639.
71 Liikanen I, Monsurrò V, Ahtiainen L, et al. Induction of interferon pathways mediates in vivo resistance to oncolytic adenovirus. *Mol Ther*. 2011;19(10):1858–1866.
72 Zheng Y, Stamminger T, Hearing P. E2F/Rb family proteins mediate interferon induced repression of adenovirus immediate early transcription to promote persistent viral infection. *PLoS Pathog*. 2016;12(1):e1005415.
73 Snaider S, Zheng Y, Hearing P. Rb-E2F-HDAC repressor complexes control interferon-induced repression of adenovirus to promote persistent infection. *J Virol*. 2022;96(11):e0044222.
74 Hajda J, Leuchs B, Angelova AL, et al. Phase 2 trial of oncolytic H-1 parvovirus therapy shows safety and signs of immune system activation in patients with metastatic pancreatic ductal adenocarcinoma. *Clin Cancer Res*. 2021;27(20):5546–5556.
75 Russell SJ, Barber GN. Oncolytic viruses as antigen-agnostic cancer vaccines. *Cancer Cell*. 2018;33(4):599–605.
76 Davola ME, Mossman KL. Oncolytic viruses: how "lytic" must they be for therapeutic efficacy? *Oncoimmunology*. 2019;8(6):e1581528.
77 Bots STF, Landman SL, Rabelink MJWE, van den Wollenberg DJM, Hoeben RC. Immunostimulatory profile of cancer cell death by the AdV-lumc007-derived oncolytic virus 'GoraVir' in cultured pancreatic cancer cells. *Viruses*. 2023;15(2):283.
78 Araki H, Tazawa H, Kanaya N, et al. Oncolytic virus-mediated p53 overexpression promotes immunogenic cell death and efficacy of PD-1 blockade in pancreatic cancer. *Mol Ther Oncolytics*. 2022;27:3–13.
79 Wang R, Chen J, Wang W, et al. CD40L-armed oncolytic herpes simplex virus suppresses pancreatic ductal adenocarcinoma by facilitating the tumor microenvironment favorable to cytotoxic T cell response in the syngeneic mouse model. *J Immunother Cancer*. 2022;10(1):e003809.
80 Derani JM. *Combining radiation and oncolytic measles virus for the treatment of refractory tumors*. 2023.
81 van de Merbel AF, Arjanneke F, van der Horst G, et al. Reovirus mutant jin-3 exhibits lytic and immune-stimulatory effects in preclinical human prostate cancer models. *Cancer Gene Ther*. 2022;29(6):793–802.
82 Liu X, Wei L, Xu F, et al. SARS-CoV-2 spike protein-induced cell fusion activates the cGAS-STING pathway and the interferon response. *Sci Signal*. 2022;15(729):eabg8744.
83 Iampietro M, Dumont C, Mathieu C, et al. Activation of cGAS/STING pathway upon paramyxovirus infection. *iScience*. 2021;24(6):102519.
84 Sato H, Hoshi M, Ikeda F, Fujiyuki T, Yoneda M, Kai C. Down-regulation of mitochondrial biogenesis by virus infection triggers antiviral responses by cyclic GMP-AMP synthase. *PLoS Pathog*. 2021;17(10):e1009841.
85 Jiang M, Chen P, Wang L, et al. cGAS-STING, an important pathway in cancer immunotherapy. *J Hematol Oncol*. 2020;13(1):81.
86 Martin NT, Bell JC. Oncolytic virus combination therapy: killing one bird with two stones. *Mol Ther*. 2018;26(6):1414–1422.
87 Kemp V, Lamfers MLM, van der Pluijm G, van den Hoogen BG, Hoeben RC. Developing oncolytic viruses for clinical use: a consortium approach. *Cytokine Growth Factor Rev*. 2020;56:133–140.